

Supporting Information for “Mechanisms of Hydrogen Bond Formation between Ionic Liquids and Cellulose and the Influence of Water Content”

Brooks D. Rabideau and Ahmed E. Ismail

January 15, 2015

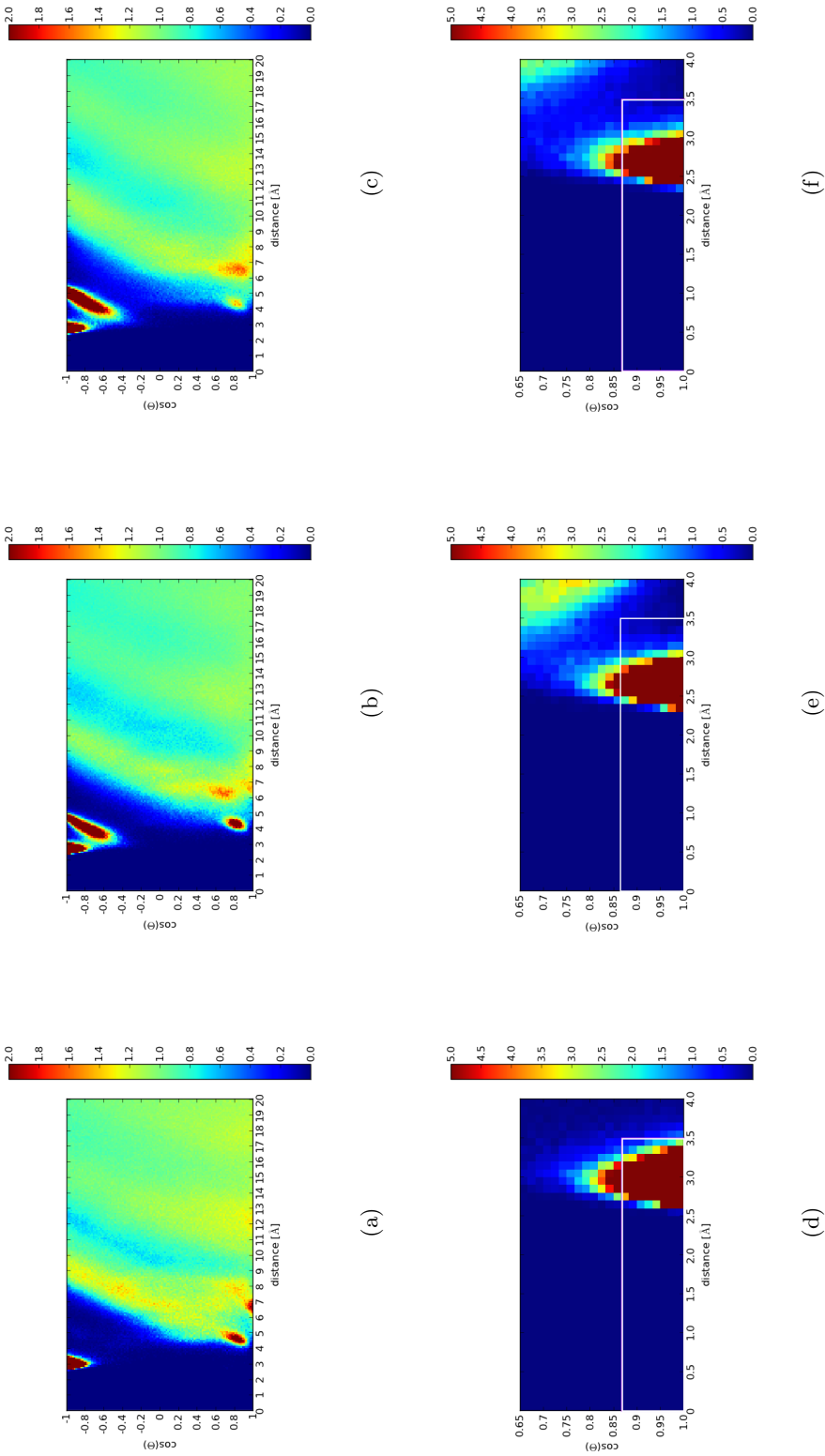


Figure 1: The $g(r, \Theta)$ distribution functions for (a) $[C_2\text{mim}]Cl$, (b) $[C_2\text{mim}]Ac$ and (c) $[C_2\text{mim}]DMP$ in which X designates either the anion oxygens or the chloride ion, r is the $O - X$ distance and Θ the HOX angle. Magnification of the main hydrogen bonding region for (d) $[C_2\text{mim}]Cl$, (e) $[C_2\text{mim}]Ac$ and (f) $[C_2\text{mim}]DMP$. The white rectangle in (d-f) indicates the cutoff criteria used in the determination of H-bonding: $r=3.5$ Å and $\Theta=30^\circ$

Table 1: Fraction of the total time spent in given transition states and the average binding lifetime of a given anion with cellulose when beginning in a give state for [C₂mim]Cl.

State	fraction of time		lifetime [ns]	
	30°	60°	30°	60°
S ₁	0.712	0.708	1.0	1.1
S ₂	0.280	0.284	3.5	3.6
S ₃	0.007	0.008	7.9	7.9
S ₄	0.000	0.000	2.5	2.5

Table 2: Fraction of the total time spent in given transition states and the average binding lifetime of a given anion with cellulose when beginning in a give state for [C₂mim]Ac

State	fraction of time		lifetime [ns]	
	30°	60°	30°	60°
S ₁	0.578	0.585	1.2	1.4
B ₁₁	0.361	0.339	5.0	5.3
S ₂	0.048	0.048	4.6	4.8
B ₁₂	0.011	0.006	7.0	5.4

Table 3: Fraction of the total time spent in given transition states and the average binding lifetime of a given anion with cellulose when beginning in a give state for [C₂mim]DMP

State	fraction of time		lifetime [ns]	
	30°	60°	30°	60°
S ₁	0.627	0.626	0.7	0.8
B ₁₁₀₀	0.279	0.275	2.7	3.5
S ₂	0.067	0.069	2.4	3.0
B ₁₂₀₀	0.015	0.014	4.2	5.5
B ₀₁₀₁	0.006	0.005	2.7	3.8
S ₁ [*]	0.004	0.004	0.6	0.9

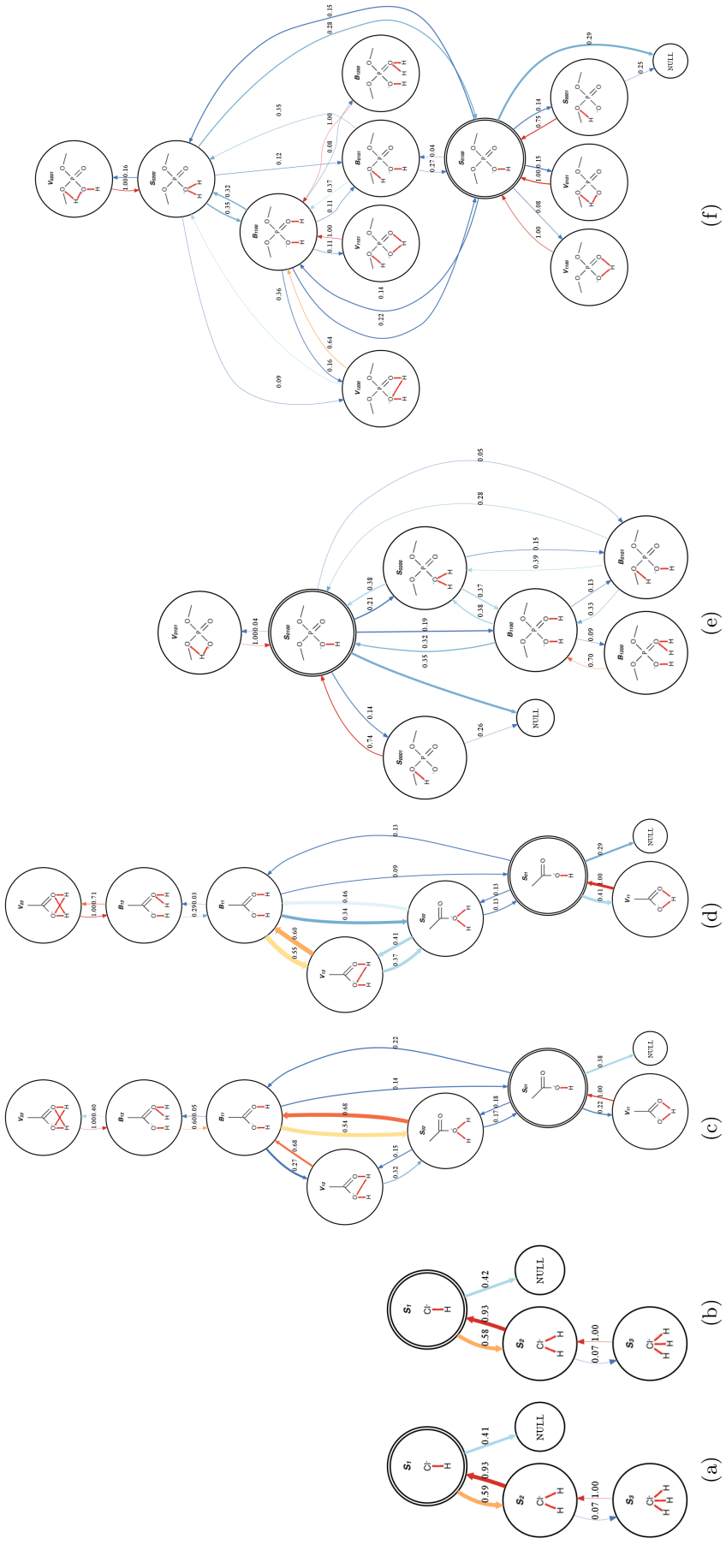


Figure 2: Transition pathways between different binding states for (a)[C₂mim]Cl with $\Theta = 30^\circ$, (b)[C₂mim]Cl with $\Theta = 60^\circ$, (c)[C₂mim]Ac with $\Theta = 30^\circ$, (d)[C₂mim]Ac with $\Theta = 60^\circ$, (e)[C₂mim]DMP with $\Theta = 30^\circ$, (f)[C₂mim]DMP with $\Theta = 60^\circ$,

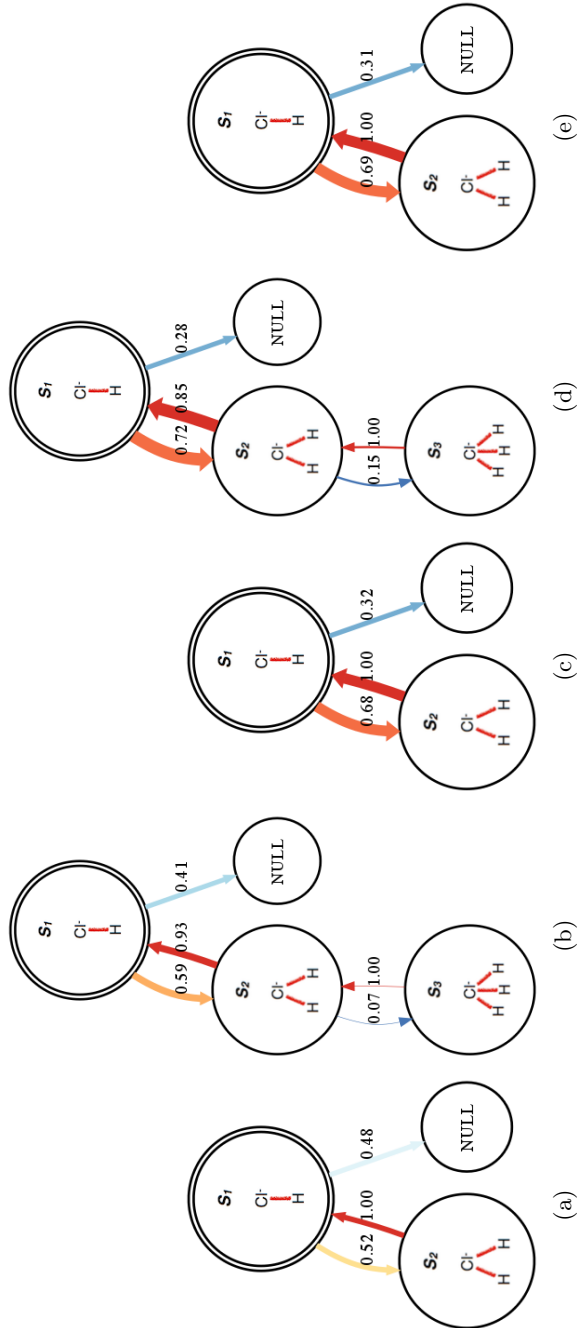


Figure 3: Transition pathways between different binding states for (a) $[C_1\text{mim}]Cl$, (b) $[C_2\text{mim}]Cl$, (c) $[C_3\text{mim}]Cl$, (d) $[C_4\text{mim}]Cl$, and (e) $[C_5\text{mim}]Cl$.

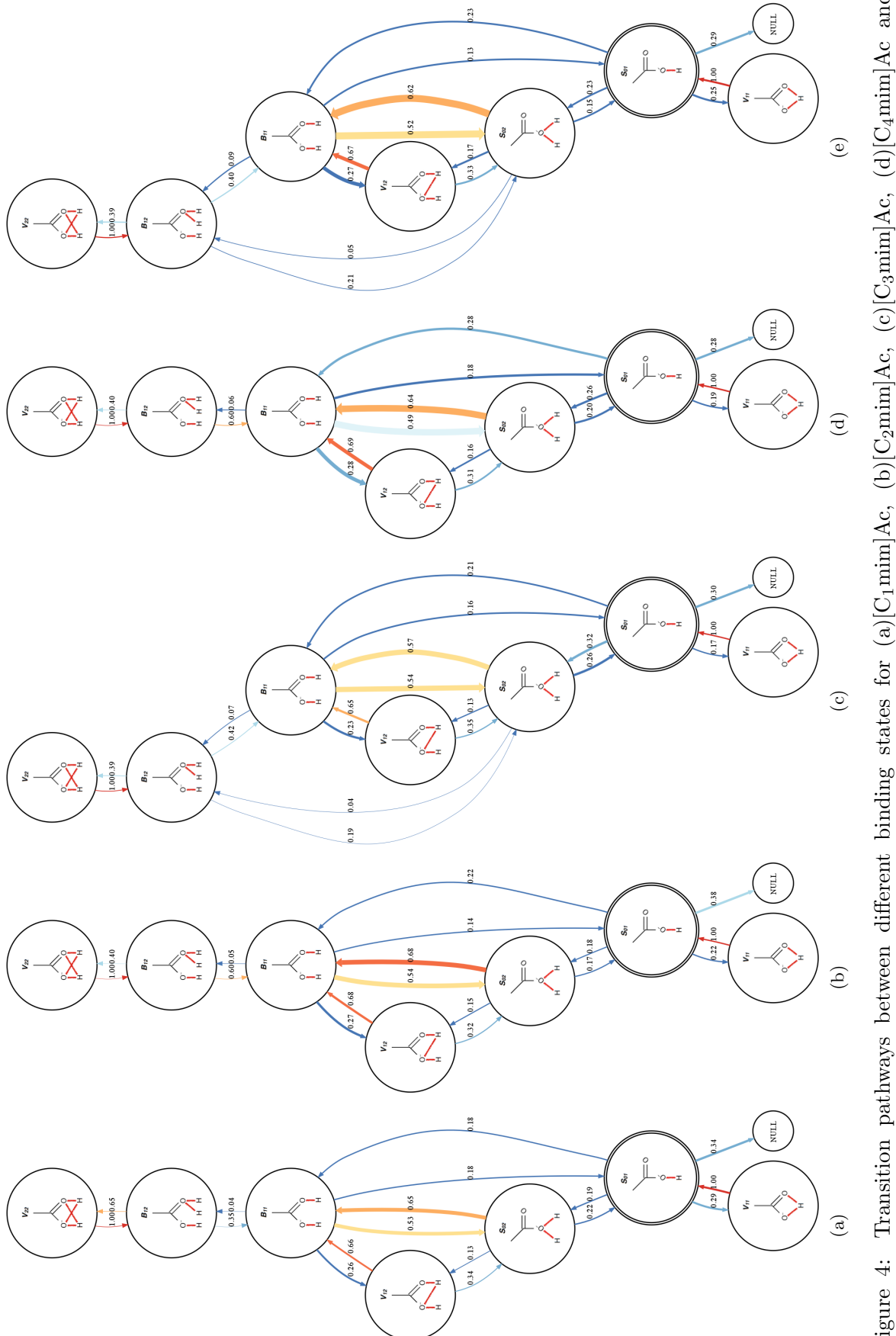


Figure 4: Transition pathways between different binding states for (a)[C₁mim]Ac, (b)[C₂mim]Ac, (c)[C₃mim]Ac, (d)[C₄mim]Ac and (e)[C₅mim]Ac,

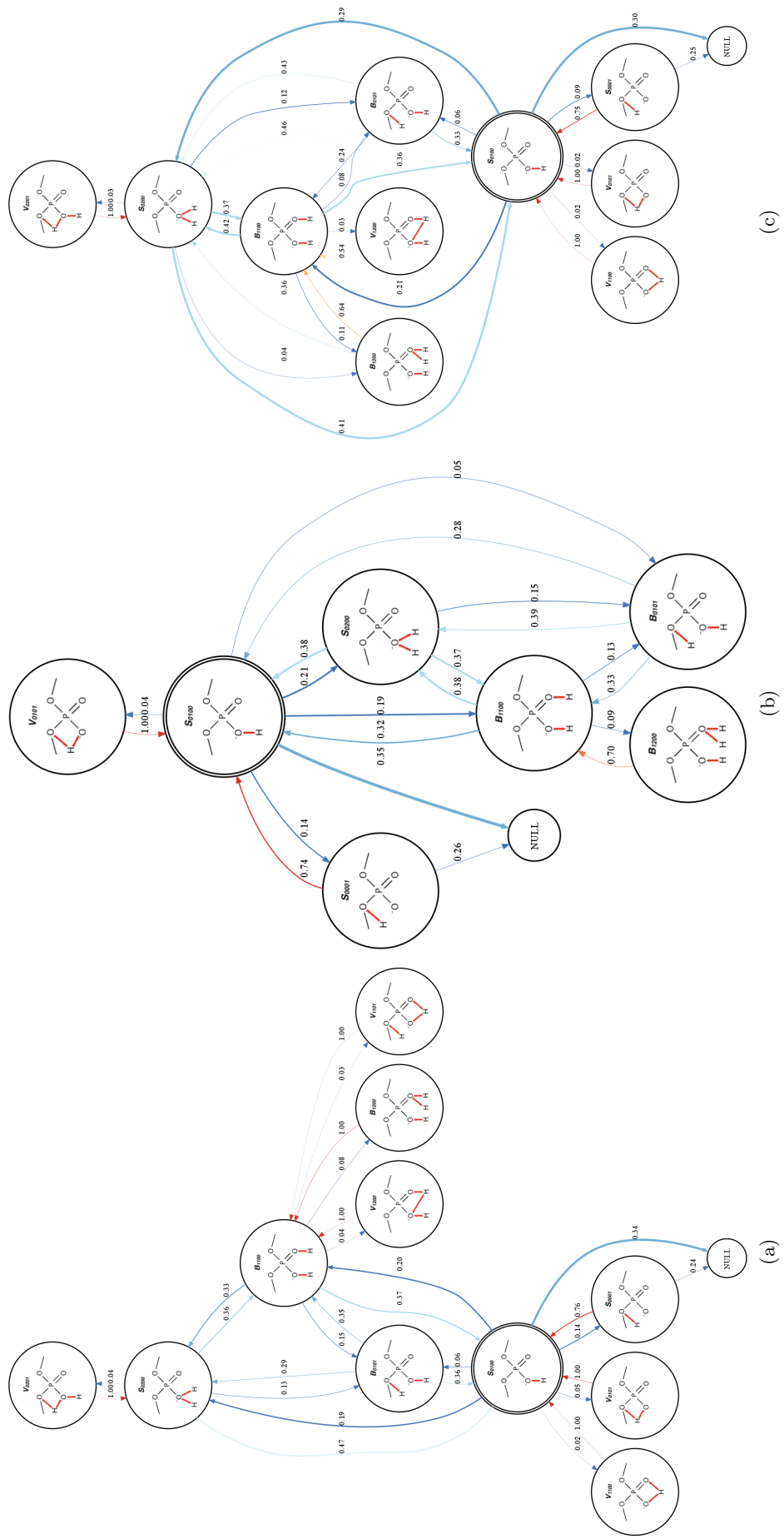


Figure 5: Transition pathways between different binding states for (a) [C₁mim]DMP, (b) [C₂mim]DMP, and (c) [C₃mim]DMP

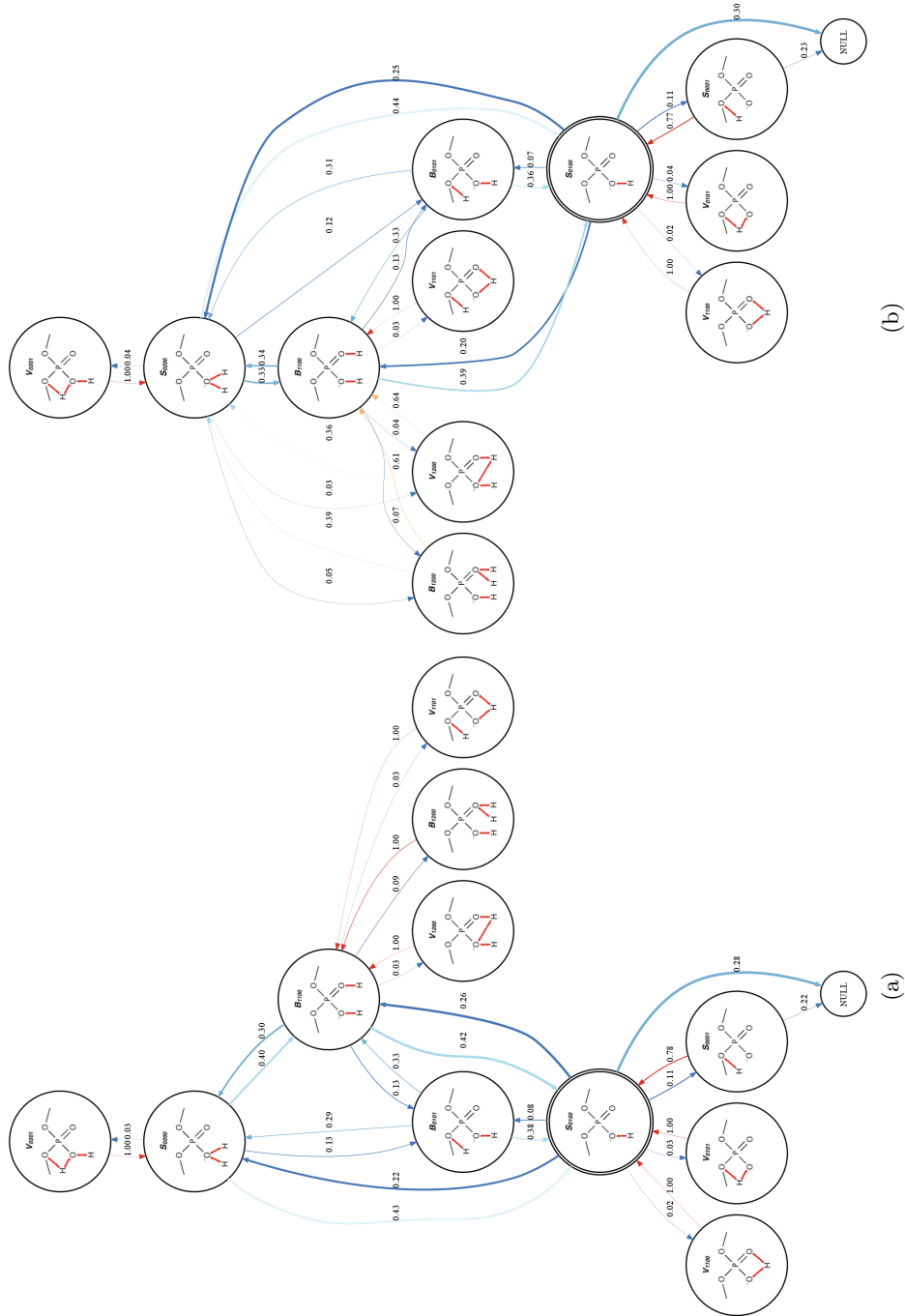


Figure 6: Transition pathways between different binding states for (d)[C₅mim]DMP and (e)[C₄mim]DMP,

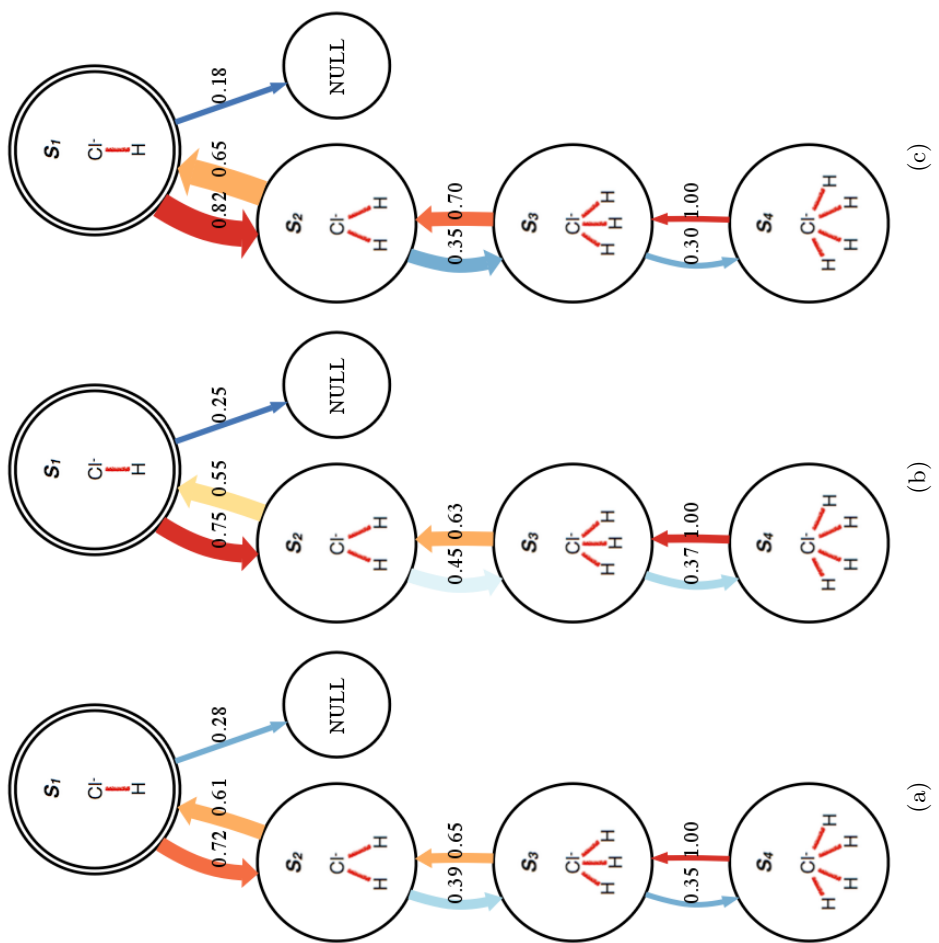


Figure 7: Transition pathways between different binding states for the cellulose bundle simulations for (a)[C₂mim]Cl, (b)[C₃mim]Cl and (c)[C₄mim]Cl

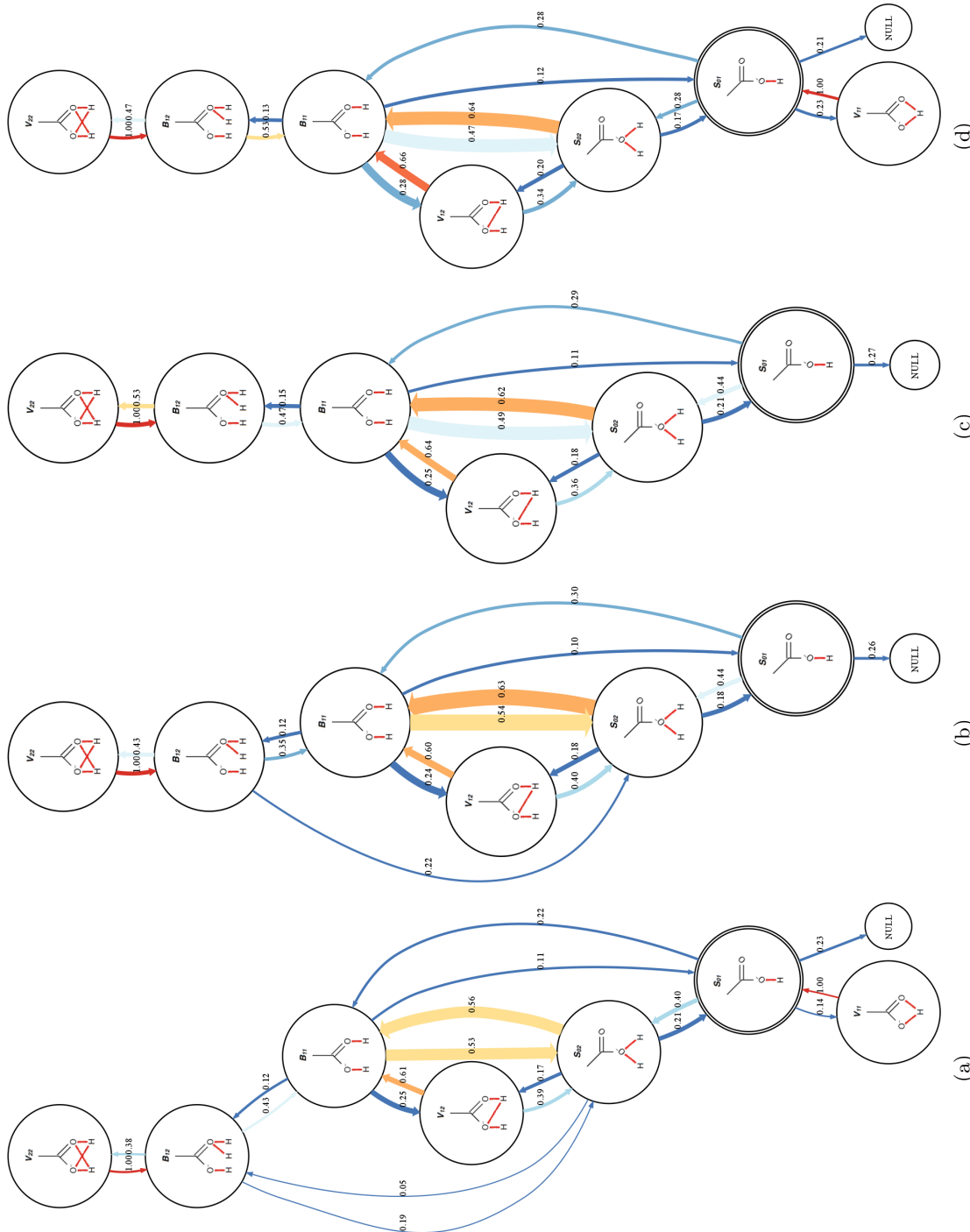


Figure 8: Transition pathways between different binding states for the cellulose bundle simulations for (a)[C₁mim]Ac, (b)[C₂mim]Ac, (c)[C₃mim]Ac and (d)[C₄mim]Ac

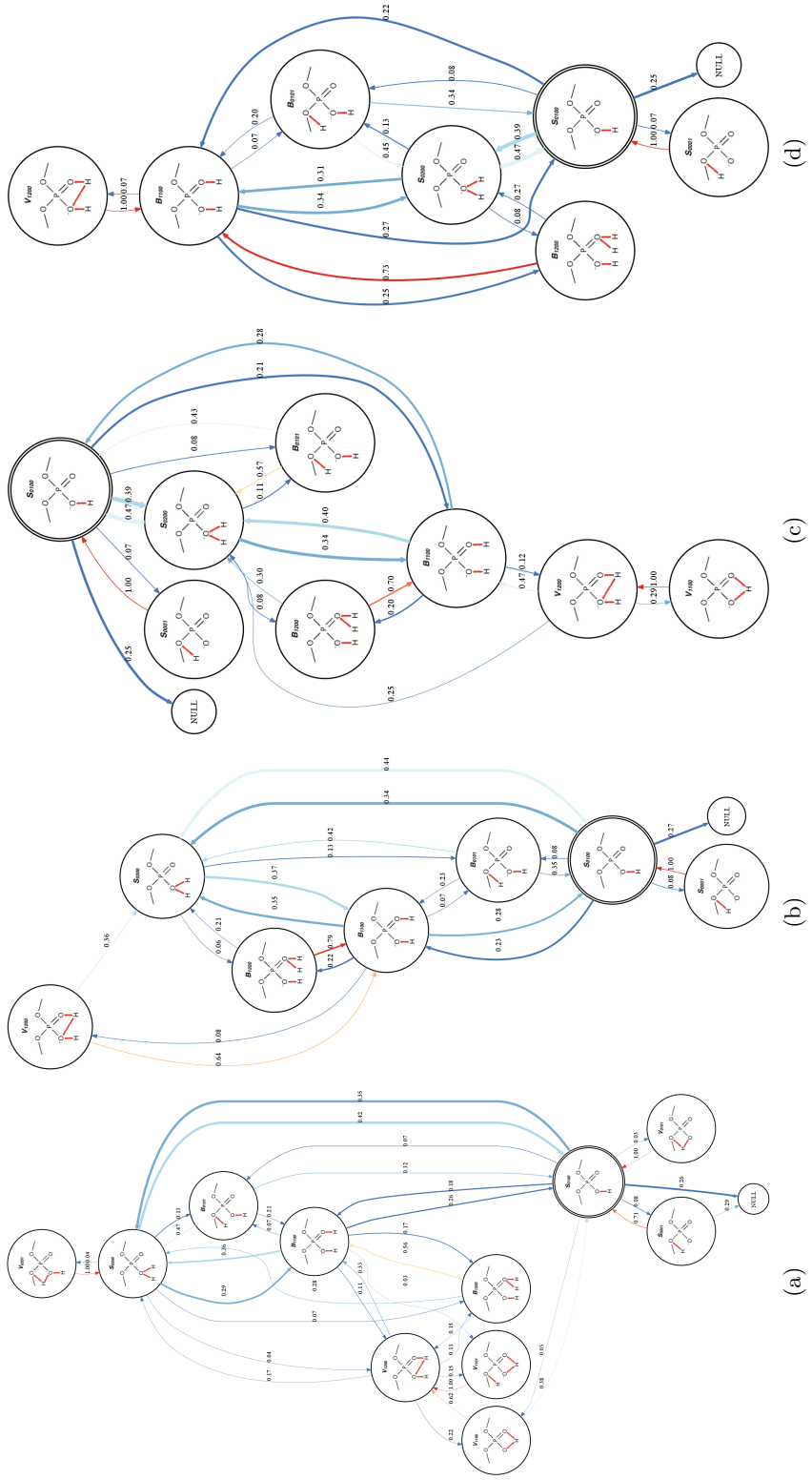


Figure 9: Transition pathways between different binding states for the cellulose bundle simulations for (a) $[C_1\text{mim}]DMP$, (b) $[C_2\text{mim}]DMP$, (c) $[C_3\text{mim}]DMP$ and (d) $[C_4\text{mim}]DMP$

Anion Motions

The mean squared angular displacement (MSAD) of anions in each of the given states were calculated according to the method of [Edmonds et. al., PNAS, 109(44), 17891-17896, 2012]. The rotational motion of a unit vector \underline{u} is determined by first determining the instantaneous axis of rotation of the vector rotation, give as the cross-product $\underline{u}(t) \times \underline{u}(t + \Delta t)$, and the magnitude of the angular displacement $\Delta\varphi(t)$, given as $|\Delta\varphi(t)| = \cos^{-1}(\underline{u}(t) \cdot \underline{u}(t + \Delta t))$. The total angular displacement then, is calculated via the integral:

$$\varphi(t) = \int_0^t \Delta\varphi(t') dt'. \quad (1)$$

The MSAD then is simply

$$\langle \Delta\varphi(\Delta t) \rangle = \langle [\varphi(t + \Delta t) - \varphi(t)]^2 \rangle \quad (2)$$

If we were to consider only one unit vector, we would likely miss some of the important rotations in 3D. Instead we consider three orthogonal unit vectors in each of the anions and average the MSADs to obtain the complete MSAD. For acetate we consider the O–O vector, the C–C vector and the cross product of these two vectors. For dimethylphosphate we consider the vector between the POO^- oxygens, the bisector of this OPO angle and the cross product of these two vectors.

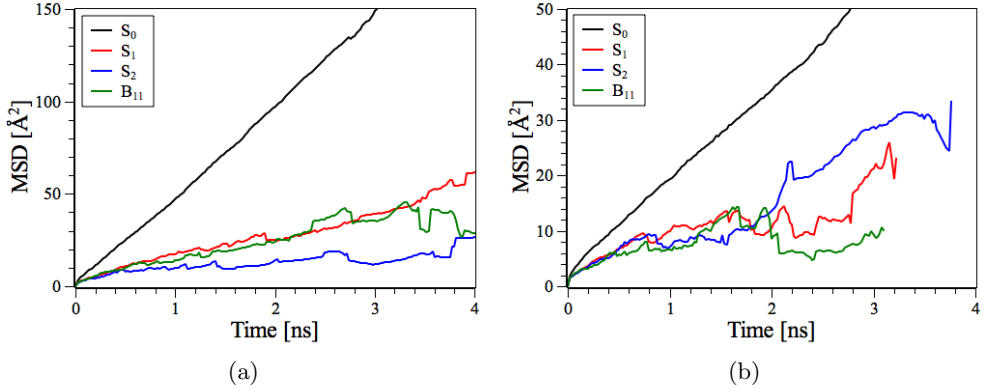


Figure 10: The mean squared displacement of the center of mass of anions belonging to a given state for (a) $[\text{C}_2\text{mim}]\text{Ac}$ and (b) $[\text{C}_2\text{mim}]\text{DMP}$.

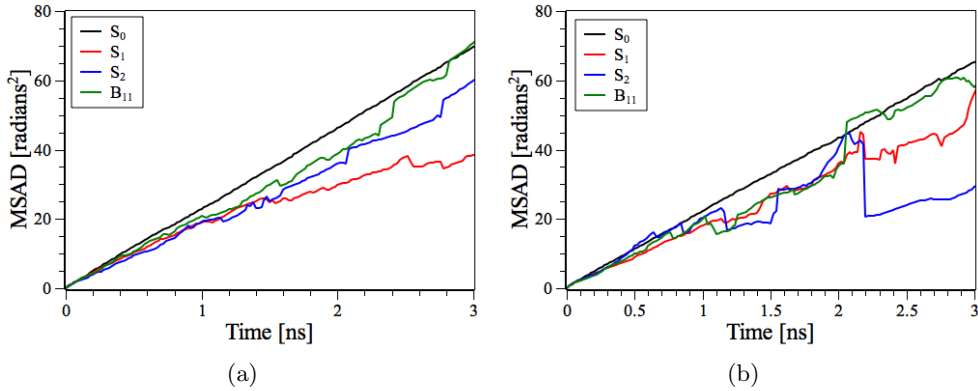


Figure 11: The mean squared angular displacement of anions belonging to a given state for (a) $[C_2mim]Ac$ and (b) $[C_2mim]DMP$.

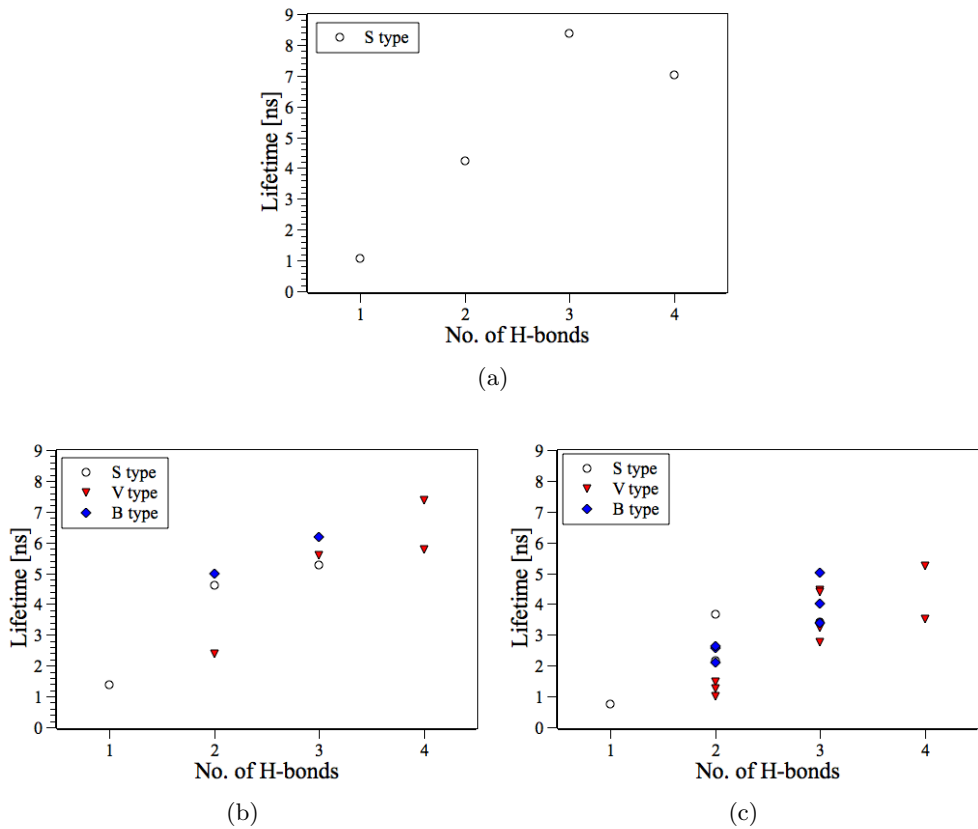


Figure 12: Average lifetimes of acetate remaining bound with cellulose when beginning in various S-, B- and V-type states for the (a) chlorides, (b) acetates and (c) dimethylphosphates.

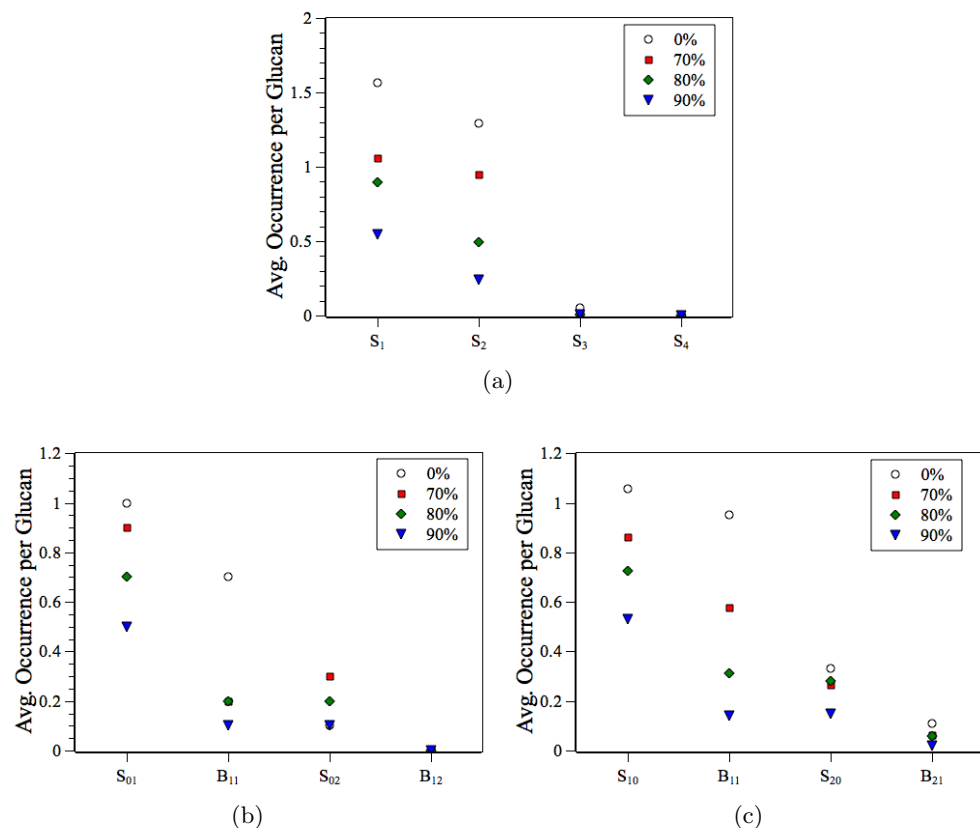


Figure 13: Average number of hydrogen bonds between (a) chloride and cellulose in [C₂mim]Cl, (b) acetate and cellulose in [C₂mim]Ac and (c) dimethylphosphate and cellulose in [C₂mim]DMP associated with the four most populous states. Values are given on a per glucan basis.

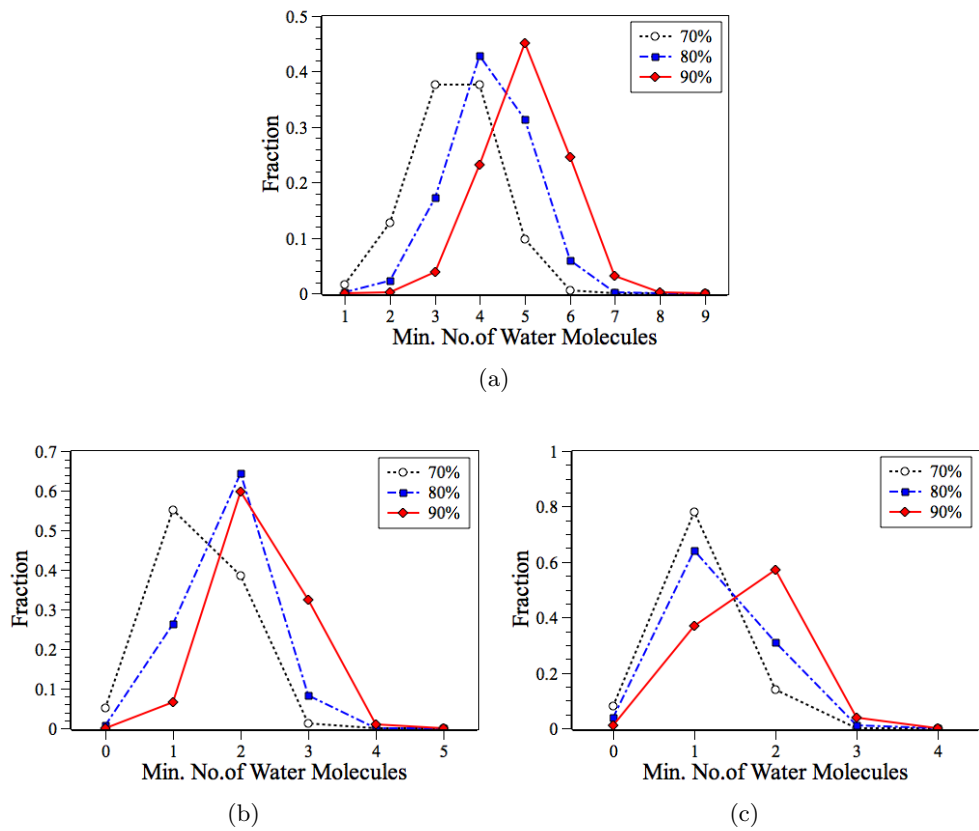


Figure 14: Fraction of free (a) chlorides, (b) acetates and (c) dimethylphosphates in [C₂mim]Cl, [C₂mim]Ac and [C₂mim]DMP, respectively, with a given minimal number of bound waters on any of the multiple H-bonding sites.